Pivotal role of duct epithelia in salivary gland GVHD

Masaru Sasaki[1][*], Yasushi Sawanobori[1][*], Toshiya Tanaka[2], Hiashi Ueta[1],
Yusuke Kitazawa[1], Sachiko Kikuta[3], Thomas B. Issekutz[4], and Kenjiro Matsuno[1]

[1]Department of Anatomy (Macro), Dokkyo Medical University, Tochigi Japan, [2]Division of Metabolic Medicine, Laboratory for System Biology and Medicine, Research Center for Advanced Science and Technology, The University of Tokyo, Tokyo, Japan, [3]Department of Anatomy and Developmental Biology, School of Medicine, Tokyo Women's Medical University, Tokyo, Japan, [4]Department of Microbiology and Immunology, Dalhousie University, Halifax, Canada.
*: These authors contributed equally.

Summary. Although salivary glands are one of the target organs in graft-versus host disease (GVHD), mechanism of disease-related tissue injury has been poorly understood. To investigate it, we employed rat GVHD model including irradiation and donor cell transfer. Immunostaining revealed that submandibular and parotid, but not sublingual glands showed acinar reduction whereas ducts were almost intact. Ductal area of sublingual glands was significantly smaller than those of submandibular and parotid glands. Ductal epithelial cells upregulated expression of class II major histocompatibility complex antigens overtime. This expression preceded donor cell infiltration. Donor cell infiltration was preferentially found in ductal area at the early phase of the disease. While ductal epithelial cells exhibited upregulated mRNA expression of Th1-type chemokines, infiltrating donor cells exhibited their receptors CXCR3 and CCR5. These results suggest ductal epithelial cells have a pivotal role in the progression of GVHD.

Address for correspondence: Sawanobori Yasushi, Department of Anatomy (Macro), Dokkyo Medical University, 880 Oaza, Kitakobayashi, Mibu, Tochigi 321-0293, Japan
Tel: +81-0282-87-2123, Fax: +81-0282-86-6229
E-mail: sawa@dokkyomed.ac.jp

Introduction

In graft-versus host disease (GVHD), salivary glands are one of the primary target organs besides skin and gastrointestinal tracts (Imanguli et al., 2010; Nagler et al., 2004), and impaired secretion of saliva affects patients' quality of life through oral filthiness, caries and decreased appetite. Although this symptom is well-known, pathophysiology and mechanism of salivary gland injury have been poorly investigated. In reports of human cases, to avoid invasive clinical examination, assessment of salivary gland lesions had been substituted with oral minor salivary glands (Alborghetti et al., 2005; Prochorec-Sobieszek et al., 2012; Soares et al., 2013). Using biopsies of minor salivary glands of oral mucosa, expression of chemokines and cytokines (Hayashida et al., 2013), infiltration of CD4-positive and CD8-positive T cells (Hiroki et al., 1996; Soares et al., 2005), and expression of HLA-DR, human class II major histocompatibility complex (MHCII) molecule on ductal epithelial cells (Hiroki et al., 1996; Lindahl et al., 1988) were assessed to date, from an immunological point of view. However, because the major salivary glands are composed of a varied mixture of serosal and mucous glands, minor glands might not always reflect pathology of three different major glands, submandibular gland (SMG), parotid gland (PG), and sublingual gland (SLG).

In humans and in most other species, MHCII is primarily

expressed on antigen-presenting cells like dendritic cells, B cells, activated T cells, macrophages, and activated endothelial cells. Human HLA-DR expression on ductal epithelial cells in salivary glands caused us to consider that ductal cells act as antigen-presenting cells to stimulate T cells to promote the disease. However, kinetics of MHCII on ductal epithelial cells and interactions between ductal cells and T cells were not studied in these human reports. Besides, expression of chemokines and cytokines had been assessed by using whole gland of surrounding oral mucosa, so it is still unclear which cells or tissue components are responsible to secrete these humoral factors in salivary glands (Hayashida et al., 2013).

In this report, we employed rat GVHD model to investigate three different major salivary glands directly, focusing on kinetics of MHCII expression on ductal epithelial cells, donor cell infiltration, and chemokine expression. Moreover, tissue damages and chemokine expression were assessed with immunohistochemistry to identify responsible cells and tissue components.

Materials and Methods

Animals

Inbred 10 weeks old male DA (RT1A^{a}B^a) rats were purchased from SLC Company (Shizuoka, Japan). 8 weeks old male Lewis (RT1A^{l}B^l) rats were purchased from Charles River Laboratories Japan, inc. (Kanagawa, Japan). Animal handling and care protocols were approved by the Dokkyo Medical University Animal Experiments Committee, and were in accordance with Dokkyo University's Regulations for Animal Experiments and with Japanese Governmental Law No. 105. To obtain tissues, all animals were killed by exsanguination from the abdominal aorta under isoflurane general anesthesia. At least three rats were used in each experiment.

Induction of GVHD and tissue collection

GVHD was induced as previously reported (Zhou et al., 2008). Briefly, recipient Lewis rats received a total body sub-lethal irradiation at a dose of 3 Gy twice with 4 hours of interval (filter: 0.5 mm aluminum + 0.1 mm copper, Hitachi MBR-1505R, Tokyo, Japan). Thoracic duct lymphocytes of

DA rats were used as donor cells. These cells were obtained by routine thoracic duct cannulation (Ford et al., 1978), and aseptically collected overnight at 4°C. Lymph was filtered with 40 μm cell strainers (Becton, Dickinson and Company, New Jersey, USA) and centrifuged at 1300 rpm for 8 minutes to collect donor lymphocytes. Collected lymphocytes were washed in PBS. One day after the irradiation, 5×10^7 lymphocytes were injected to recipient rats intravenously. By this procedure, GVHD was induced in recipient rats with mean survival time of 9.83 ± 0.75 days. Lewis rats with/ without irradiation and without donor cell injection were defined as irradiated control and untreated rats respectively. Recipient rats were sacrificed at 2–10 days after cell transfer and tissues were collected. Before sacrifice, Bromodeoxyuridine (BrdU) (6 mg/ 200 g body weight, Sigma-Aldrich Japan, Tokyo) was injected intravenously to label proliferating cells. Collected tissues were frozen freshly, or after fixation in periodate-lysine-paraformaldehyde (PLP: 0.1 M lysine hydrochloride, 0.01 M sodium periodate and 1% paraformaldehyde in PBS). In brief, tissues were cut into 5–10 mm pieces and rotated gently in PLP solution overnight at 4°C, followed by sucrose infiltration. Sucrose infiltration was performed with incubation in 10, 20, 30% sucrose-PBS for 4 hours-overnight respectively. After sucrose infiltration, tissues were frozen for cryosectioning.

Antibodies and Reagents

The primary and secondary antibodies used for immunohistology are listed in Table 1. A monoclonal antibody clone B12 against anti-type IV collagen-like molecule was kindly donated by Dr. T. Ezaki.

Immunohistochemistry and statistical analysis of areas or cell numbers

For tissue preparation, optimal conditions were predetermined by preliminary experiments. Briefly, freshly frozen sections were used to stain keratin 5 (Fig. 1), MN (Fig. 3), and CXCR3 (Fig. 4l, m), and PLP-fixed sections were used to stain CXCL9, CXCL10, CCL5, and CCR5 (Fig. 4a–k, n, o). In cases of freshly frozen tissues, cryosections were fixed with acetone and rehydrated in TBS buffer. Then sections were fixed again with formol-calcium solution briefly. In case of PLP fixed tissues, sections were simply

Table 1 Antibodies used in this research

Antigen	Isotype	Clone	Source
keratin 5	rabbit IgG	polyclonal	a
recipient MHCII (RT1B[i])	mouse IgG$_1$	OX3	b
BrdU	rat IgG$_{2a}$	BU1/75	c
donor MHC I (RT1A[a])	mouse IgG$_1$	MN$_{4-91-6}$	b
CXCL9	rabbit IgG	polyclonal	d
CXCL10	rabbit IgG	polyclonal	e
CCL5	rabbit IgG	polyclonal	f
CXCR3	armenian hamster IgG	XR3.2	g
CCR5	rat IgG$_{2a}$ (FITC conjugated)	HEK/1/85a	h
ICAM-1	mouse IgG$_1$	1A29	i
type IV collagen	rabbit IgG	polyclonal	j
type IV collagen like molecule	mouse IgG	B12	k

2nd antibodies

product	conjugate	source
goat anti-mouse IgG	alkaline phosphatase	l
rabbit anti-mouse IgG	peroxidase	m
donkey anti-rat IgG	alkaline phosphatase	n
donkey anti-rabbit IgG	alkaline phosphatase	n
goat F(ab')2 to rabbit Ig	peroxidase	o
goat anti-armenian hamster IgG	alkaline phosphatase	n
sheep anti-FITC	alkaline phosphatase	p

[a] Assay Biotechnology (Sunnyvale, CA, USA), [b] ECACC, [c] AbD Serotec (Kingston, UK), [d] Novus Biologicals (Colorado, USA), [e] PeproTech (New Jersey, USA), [f] LSBio (Washington, USA), [g] generously provided by TB. Issekutz, [h] Abcam (Cambridge, UK), [i] Thermo Fisher Scientific (Massachusetts, USA), [j] generously provided by Dr. Y. Sado, [k] generously provided by Dr. T. Ezaki, [l] SIGMA-Aldrich (Missouri, USA), [m] DAKO (Glostrup, Denmark), [n] Jackson Immunoresearch (Pennsylvania, USA), [o] MP Biomedicals (California, USA), [p] Roche (Basel, Switzerland), ,

hydrated in PBS. All hydrated sections were immunostained as described previously (Kitazawa et al., 2015; Sawanobori et al., 2014). Briefly, molecules of interest were stained blue using alkaline phosphatase-conjugated secondary antibodies and Vector Blue substrate (Vector Laboratories, Burlingame, CA, USA). Additionally, type IV collagen, which reveals the framework of tissues, was stained brown with a peroxidase-conjugated secondary antibody and 3,3'-diaminobenzidine substrate (Dojindo Molecular Technologies, Kumamoto, Japan). On certain samples, incorporated BrdU was stained red with anti-BrdU antibody followed by alkaline phosphatase-conjugated anti-rat IgG secondary antibody and New Fuchsin (DAKO, Glostrup, Denmark), after partial digestion with pepsin (Wako Pure Chemical Industries, Osaka, Japan) solution (0.003% pepsin, 0.01 N HCl) at 37°C for 10 minutes, genome DNA fragmentation in 4 N HCl for 30 minutes, and neutralization in 180 mM $Na_2B_4O_7$ solution (pH 8.5) for 4 minutes. Photomicrographs were captured with a Microphot-FX microscope (Nikon, Tokyo, Japan) and a DP26 digital camera (Olympus, Tokyo, Japan). For calculation of acinar, stromal, and ductal areas, and number of infiltrated donor cells, annotations were drawn into each area of captured

Table 2 Primers and probes used for qPCR

Gene		Primers	Universal Probe
Actb	Forward	cccgcgagtacaaccttct	#17
	Reverse	cgtcatccatggcgaact	
Cxcl9	Forward	tgaagtccgttgctctattcc	#105
	Reverse	ggagcatcgctgattcctta	
Cxcl10	Forward	atgaacccaagtgctgctgt	#13
	Reverse	gtctcagcgtctgttcatgg	
Ccl3	Forward	gcgctctggaacgaagtct	#40,
	Reverse	gaatttgccgtccataggag	
Ccl4	Forward	ctctgcgtgtctgccttct	#63
	Reverse	tgggagggtcagagcctatt	
Ccl5	Forward	ctcaccgtcatcctcgttg	#16
	Reverse	gagtggtgtccgagccata	
Ccl20	Forward	ggggtactgctggcttacct	#71
	Reverse	ggcagcagtcaaagttgctt	

images. Each area was further calculated with Photoshop software (Adobe, California, USA). Statistical analysis was performed using the Student t-test.

Quantitative PCR (qPCR)

For RNA extraction, freshly frozen SMGs were cryosectioned, and then sections of total 150 μm thicknesses were dissolved into 800 μl of ISOGEN (Nippon Gene, Tokyo, Japan). The RNA was extracted following manufacturer's instruction. To accomplish high purity, RNA samples were dissolved into ISOGEN again and extraction procedures were repeated. After that, concentrations of RNA samples were assessed with Nanodrop (Thermo Fisher Scientific, Massachusetts, USA). Certain amount of RNA was reverse transcripted to cDNA using PrimeScript™ Reverse Transcriptase (TakaraBio, Shiga, Japan).

To perform qPCR, primer sets were designed with Universal ProbeLibrary Assay Design Center web page (https://qpcr.probefinder.com/organism.jsp). Designed primers were ordered and synthesized by Hokkaido System Science (Hokkaido, Japan) (table 2). PCR reaction mixture was prepared mixing these primer sets, Universal Probes (Roche, Basel, Switzerland), cDNA samples, and FastStart Universal Probe Master mix (Rox) (Roche). qPCR reaction was performed on StepOne™ realtime PCR system (Thermo Fisher Scientific). Data were calculated with ddCt method to obtain mRNA copy number ratio of genes of interest against beta actin.

DNA microarray

For microarray analysis, total RNA was extracted from freshly frozen SMGs as above. Then genome-wide transcription analysis was performed using GeneChip® Rat Gene 2.0 ST Array and GeneChip scanner 3000 (Affymedrix, California, USA) as described preciously (Tanaka et al., 2014).

Results

Injury and MHCII expression of salivary gland occurred in serosal glands uniquely but not in mucosal glands

Firstly, we collected major salivary glands from GVHD or irradiated control rats and immunohistologically stained to assess tissue injury accompanying the development of GVHD (Fig. 1, 2). We used anti-keratin antibody because keratin 5 (K5) is expressed in myoepithelial cells of salivary
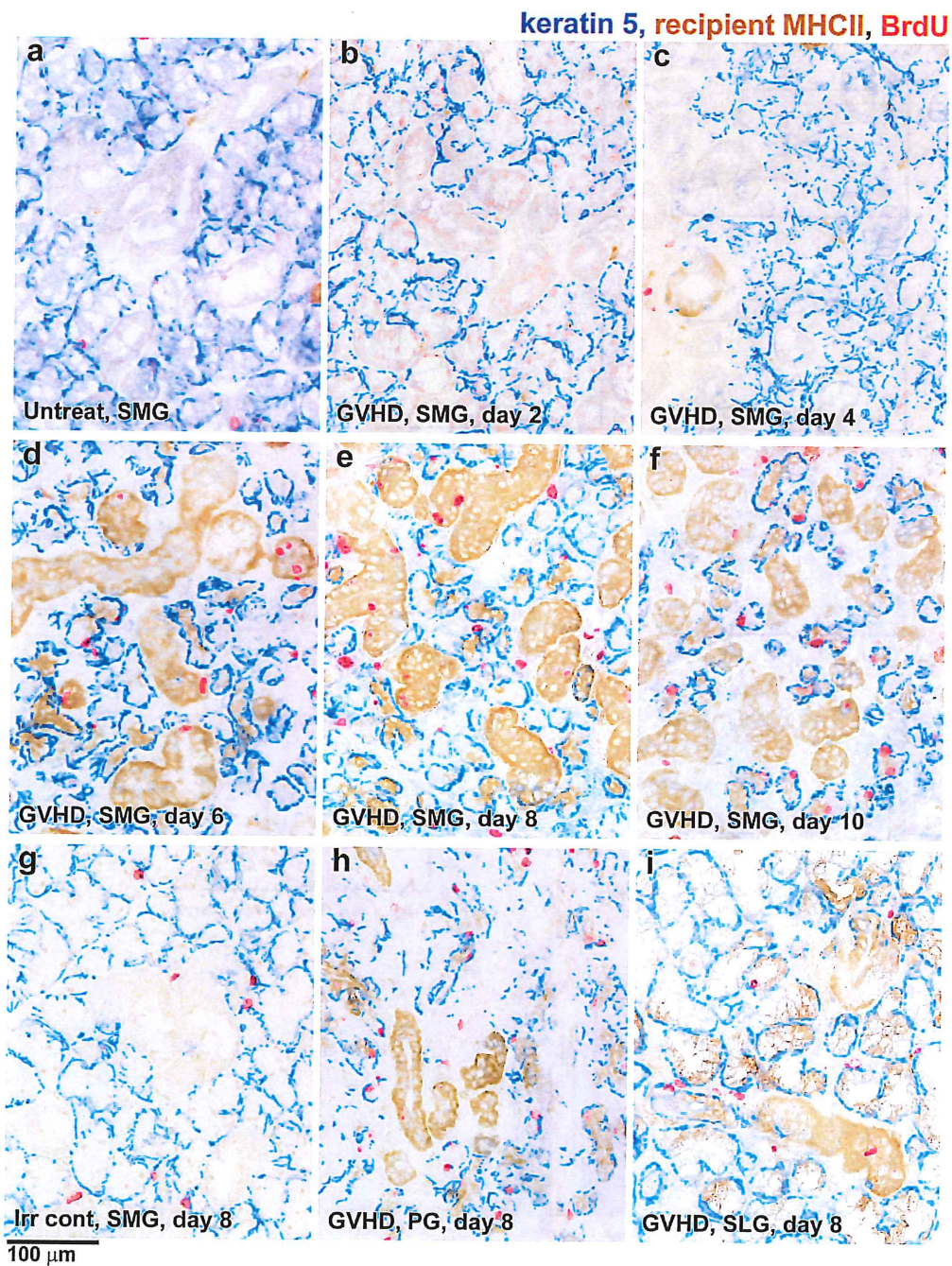
Fig. 1. Acinar damage and MHCII expression on ductal epithelial cells in GVHD-affected salivary gland. 4 μm fleshly frozen cryosections of SMGs (a–g), PGs (h), and SLGs (i) of untreated (a), irradiated control (g), and GVHD (b–f, h, i) rats were immunostained. Salivary glands were collected at 8 weeks old (a) or day 2 (b), day 4 (c), day 6 (d), day 8 (e, g–i), and day 10 (f) after donor cell transfer. In all sections, keratin 5, recipient MHCII, and BrdU were colored with Vector Blue (blue), DAB (brown), and New Fuchsin (red) substrates respectively.
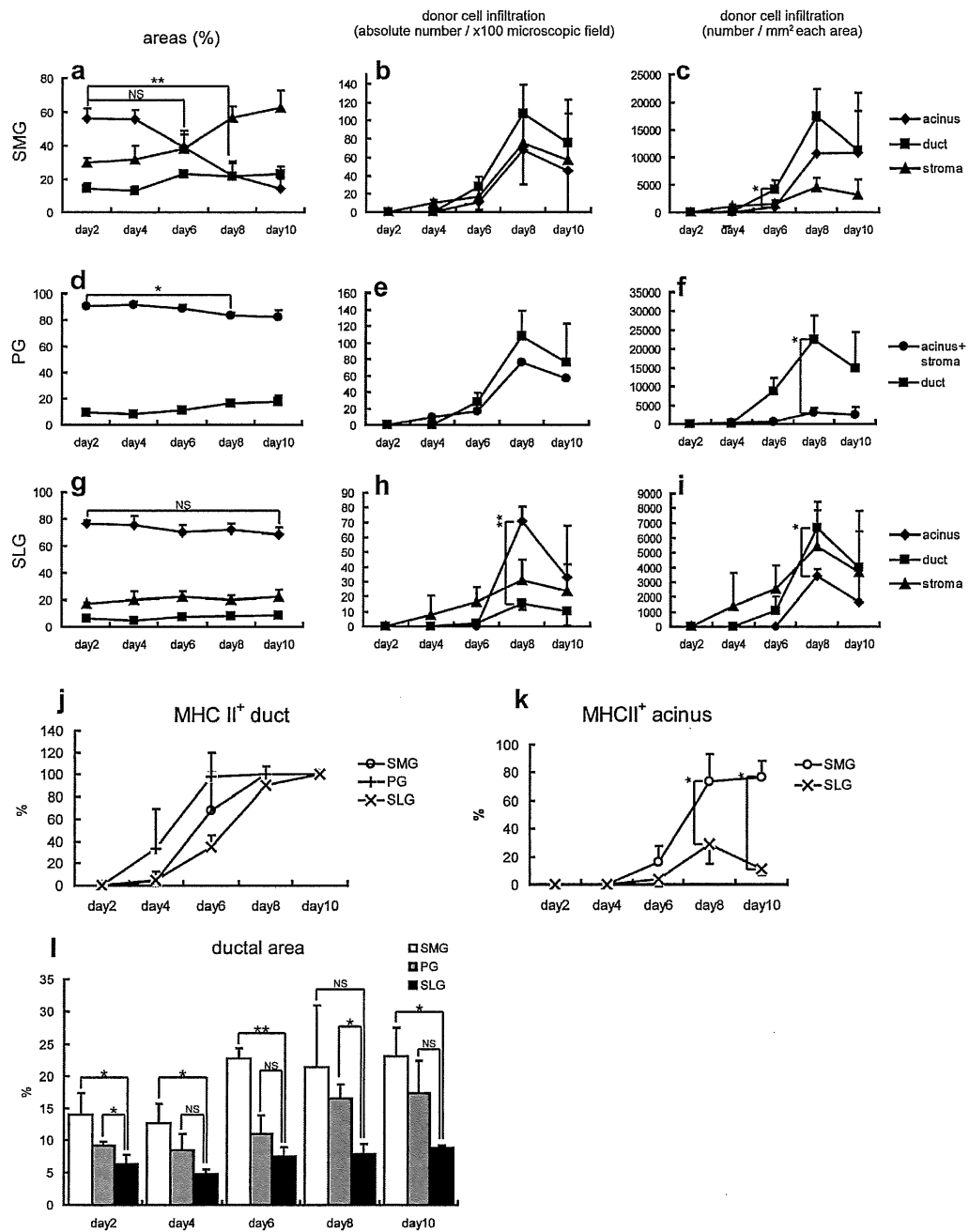
Fig. 2. Kinetics of tissue damage and donor cell infiltration in GVHD-affected salivary glands. On immunostained sections of salivary glands of GVHD rats, kinetics of each area (a, d, g), infiltrating cells (absolute number: b, e, h, concentration: c, f, i), and MHCII expression of ductal (j) or acinar (k) areas were counted and calculated. Data of ductal areas were extracted from a, d, and g for comparison (l). Sections were stained as mentioned in Figure 1 (a, d, g, j, k) or Figure 3 (b, c, e, f, h, i). At each time point, sections from 3 rats were immunostained, and at least 3 pictures were taken from 1 section for cell counting and area assessment (*: $p < 0.05$, **: $p < 0.005$, NS: not significant).

glands (Fiaschi et al., 2011; Nelson et al., 2013; Raimondi et al., 2006), thus instrumental for identification of acini. After day 6, in SMGs, K5-surrounded acini began to shrink significantly with an increase of stroma (Fig. 1b–f, Fig. 2a), whereas SLG did not show significant decrease of acini (Fig. 1i, Fig. 2g). In the case of the PG, it was difficult to distinguish acini and stroma even in untreated control rats because K5$^+$ myoepithelial cells surround acini incompletely. Accordingly, we did not discriminate acini and stroma and performed quantification of the sum of both areas in the PG study. Significant decrease of the sum areas of acini and stroma was observed, suggesting acinar damage (Fig. 1h, Fig. 2d).

Ducts in PGs and SMGs exhibited MHCII expression occurred between day 4 and day 6 (Fig. 2j), and reached virtually 100% by day 8. Therefore acinar involution and donor cell infiltration (Fig. 2a–i) was preceded by MHCII expression of ductal epithelial cells. SLGs exhibited delayed expression of MHCII compared to SMGs and PGs. In severely injured SMGs, acini also expressed MHCII and its frequency was significantly higher than that of SLGs (Fig. 2k). Acini in injured PGs also might expressed MHCII but we omitted it from Fig. 2k because of difficulty in discrimination. Noteworthy, ductal areas in SMGs and PGs were significantly broader than that of SLGs partly (Fig. 2l).

We also analyzed extraorbital lacrimal glands but they exhibit minimal acinar involution and delayed MHCII expression (data not shown).

Donor cell Infiltration into salivary glands

To assess donor cell infiltration into salivary gland lesions, we immunohistologically stained salivary glands of GVHD and irradiated control rats with anti-donor MHCI antibody (Fig. 3). MHCI is expressed on virtually all nucleated cells and has haplotypes unique to each strains, so that DA rat MHC I-specific antibody can exclusively stain donor cells. In fact, in irradiated control rats, no donor MHC I staining was observed (Fig. 3g). From day 4, donor cells started to infiltrate into SMGs of GVHD (Fig. 3b–f), PG also showed a massive donor cell infiltration (Fig. 3h), whereas SLG showed a relatively moderate infiltration (Fig. 3i). To analyze kinetics and localization of infiltration, we counted the number of donor cells within three different areas (acinus,

duct, stroma) (Fig. 2b, c, e, f, h, i). In case of SMGs, infiltration started around day 4 and reached peak around day 8, and there was no significant difference among each area when absolute numbers of donor cells were counted (Fig. 2b). However, when density of donor cells within each area was calculated, that in ducts was significantly higher than that in acini on day 6 (Fig. 2c). It was the same with the PGs when duct was compared with the sum of acini and stroma (Fig. 2e, f). In SLGs, absolute numbers of infiltrating donor cells in ducts were significantly smaller than acini (Fig. 2h). However, because SLGs have narrower ductal area, the donor cell density was significantly higher in ducts than acini (Fig. 2i). These findings suggested that duct cells attracted donor lymphocytes primarily in all these major salivary glands during the early stage of the disease.

Chemokine mRNA expression profile of SMGs

To assess the chemokine expression of SMG, total RNA was extracted from SMGs of irradiated control or GVHD rats at day 8, then microarray analysis was carried out. To analyze microarray data, we focused on MHCII genes and chemokines which act on Th1/Th2 type T cells (Mantovani et al., 2006). As a result, upregulation of MHCII gene expression was detected (table 3). Moreover, Th1 chemokines, especially ligands for CXCR3 (CXCL9, CXCL10, CXCL11), CCR5 (CCL3, CCL4, CCL5), and CCR6 (CCL20) expressed intensively. Th2 chemokine upregulations were not observed significantly (not shown). For further confirmation, qPCR was carried out (Fig. 4a). Primers for Th1 chemokines were designed (except for CXCL11: because primer set for this gene can not be designed with Universal Probe Library). Although GVHD rats exhibited 2-500 folds mRNA expression compared to irradiated control rats, only CCL3 and CCL5 were statistically significant because of the broad dispersion of data.

Chemokine protein expression in ductal epithelial cells

To identify areas expressing chemokines, sections of SMGs were stained with anti-CXCL9, anti-CXCL10 and anti-CCL5 antibodies (Fig. 4b–k). All these chemokines were expressed in duct epithelia of both GVHD and irradiated control SMGs, suggesting constitutive expression. However,
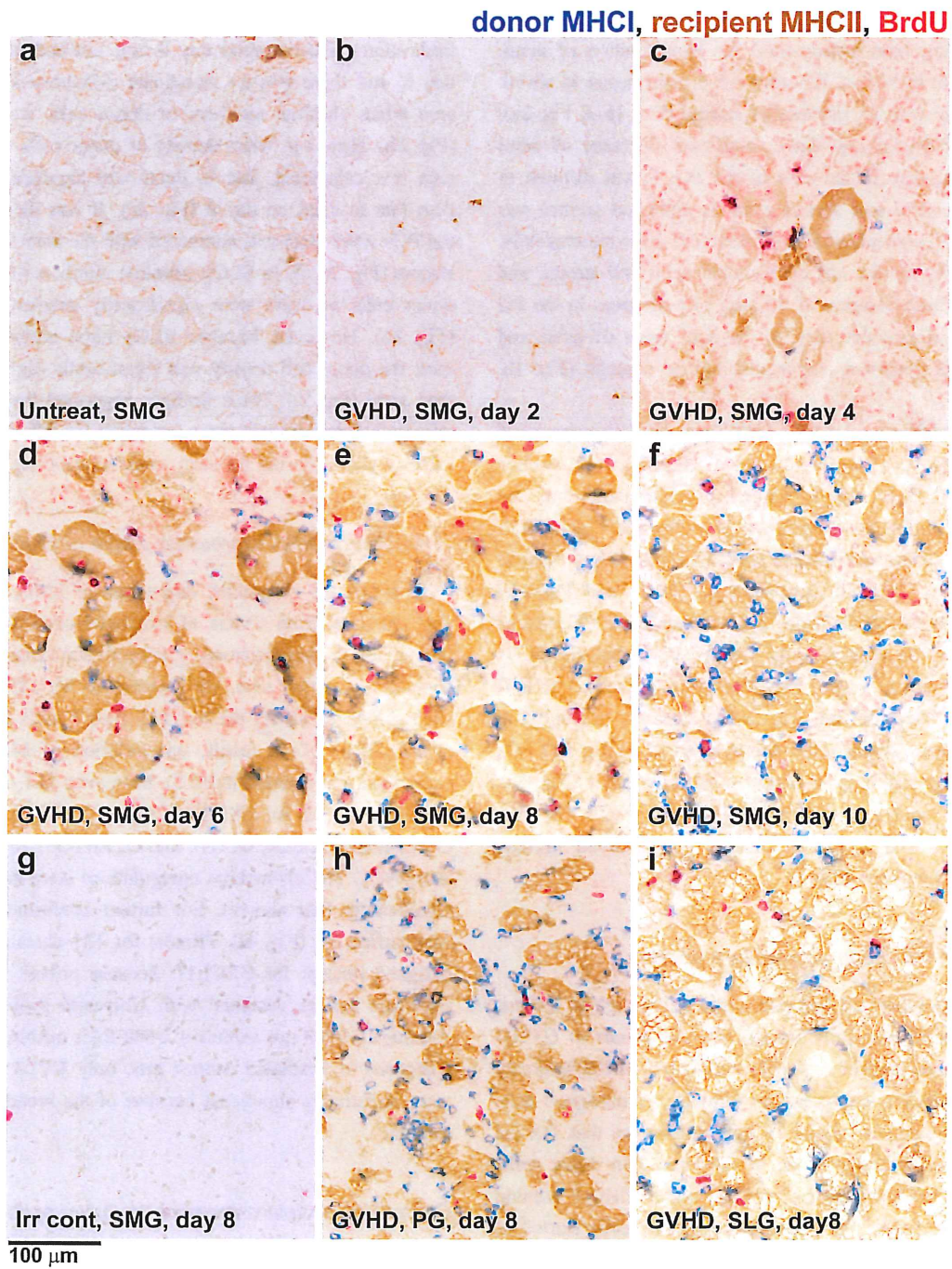
Fig. 3. Donor cell infiltration in GVHD-affected salivary gland. 4 μm fleshly frozen cryosections of SMGs (a–g), PGs (h), and SLGs (i) of untreated (a), irradiated control (g), and GVHD (b–f, h, i) rats were immunostained. Salivary glands were collected at 8 weeks old (a) or day 2 (b), day 4 (c), day 6 (d), day 8 (e, g–i), and day 10 (f) after donor cell transfer. In all sections, MN (donor MHCI), recipient MHCII, and BrdU were colored with Vector Blue (blue), DAB (brown), and New Fuchsin (red) substrates respectively.

Table 3 Changes of gene expression observed in DNA microarray experiment

affymetrix Probe_id	description	GVHD/irradiated control ratio	rank among total 31099 genes
	MHC class II		
1370822_at	RT1-Ba	25.13	69
1371033_at	RT1-Bb	107.60	10
1370883_at	RT1-Da	109.31	9
1370382_at	RT1-Db1	44.28	38
1370383_s_at		16.15	119
	Th1 chemokines receptors and chemokines		
1382454_at	CXCL9	68.89	19
1387969_at	CXCL10	92.61	13
1379365_at	CXCL11	92.83	12
1369633_at	CXCL12	5.27	685
1369815_at	CCL3	4.97	762
1370832_at	CCL4	5.36	660
1369983_at	CCL5	26.99	64
1368200_at	CX3CL1	2.41	2835
1369814_at	CCL20	22.52	83

staining of CXCL9 and CXCL10 in GVHD SMGs exhibited more intense and focal staining pattern at day 8 (Fig. 4e, h), possibly correlating with upregulation of mRNA, whereas irradiated control SMGs were weak and homogenous (Fig. 4c, f). In contrast, CCL5 staining pattern was the same in both groups at day 8 (Fig. 4i, k), although CCL5 mRNA was upregulated (Fig. 4a and table 3).

Next, we stained day 8 GVHD SMGs with anti-CXCR3 or anti-CCR5 antibodies (Fig. 4l–o). In both cases, chemokine receptor expressing cells were found to associate with ducts.

Discussion

In this report, we found: 1. Recipient MHCII molecules are expressed on ductal epithelial cells of all three major salivary glands under GVHD conditions. 2. Recipient MHCII expression precedes acinar damage and donor cell infiltration. 3. Donor cell infiltration occurred primarily in ducts. 4. Ductal epithelial cells express Th1 chemokines as well as MHCII. 5. Infiltrating donor T cells associating with ducts express Th1 chemokine receptors.

Expression of recipient MHCII on duct cells during the early stage of GVHD has been reported in bile duct (Takacs et al., 1985), but not in major salivary glands so far. However, there are several studies reporting that interferon-gamma induced expression of MHCII on epithelial tissues including salivary gland ductal cells (Steiniger et al., 1989; Steiniger et al., 1988). Many studies report secretion of interferon-gamma during GVHD progression (Wang et al., 2009; Yang et al., 2005), also in our model, where interferon-gamma was upregulated assessed with microarray (not shown). On the other hands, MHCII expression on ductal epithelial cells of salivary glands was also reported in human Sjögren's syndrome (Takaya et al., 1990) and in its mouse model (Hayashi et al., 1996). Especially in the mouse model, MHCII expression precedes progression of inflammation in accordance with our result, suggesting MHCII-positive duct may play some role in enhancing inflammatory responses. In fact, BrdU-positive donor cells found in ductal epithelia
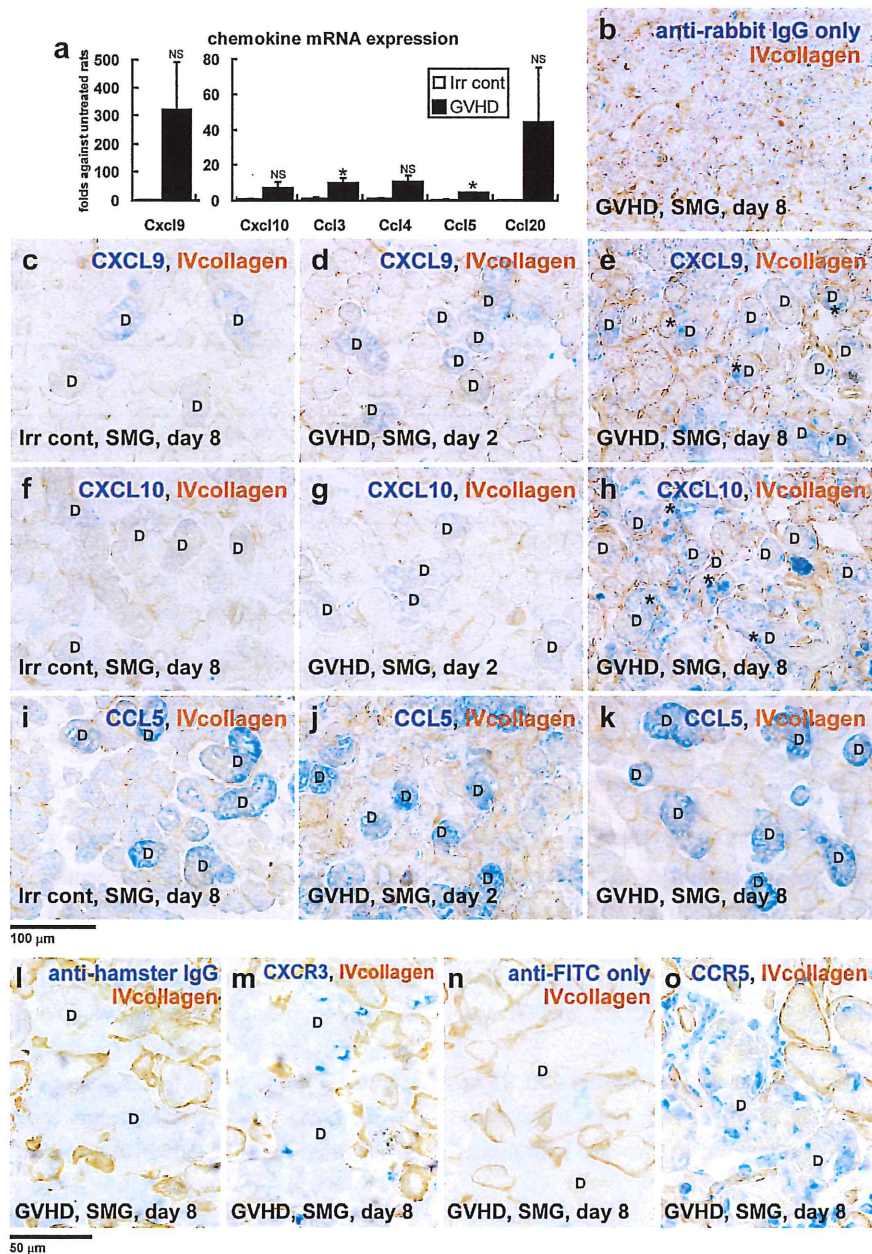
Fig. 4. Chemokine expression of ductal epithelial cells in GVHD-affected salivary glands, and receptor expression on infiltrating donor cells. **a:** qPCR was performed and data were presented as relative value against untreated rats (*: $p < 0.05$, NS: not significant). **b–k:** 6 μm PLP-fixed cryosections of SMGs of GVHD (b, d, e, g, h ,j, k) or irradiated control rats were immunostained. Tissues were collected at day 2 (d, g, j) or day 8 (b, c, e, f, i, k) after donor cell transfer. Chemokines (null: b, CXCL9: c–e, CXCL10: f–h, CCL5: i–k) and type IV collagen were colored with Vector Blue (blue) and DAB (brown) substrates respectively. Asterisks indicate focal staining patterns. "D"s in the pictures indicate ducts. **l–o:** 6 μm freshly frozen (l, m) or PLP-fixed (n, o) cryosections of SMGs of day 8 GVHD rats were immunostained. Chemokine receptors (null: l, n, CXCR3: m, CCR5: o) and type IV collagen were colored with Vector Blue (blue) and DAB (brown) substrates respectively. "D"s in the pictures indicate ducts that were not outlined by type IV collagen.

suggested donor cell activation. However, our experimental model did not show intense injury of lacrimal glands, which was found in human Sjögren's syndrome. Like SLGs, rats extraorbital lacrimal glands have relatively narrow ductal area (2.5–5%, data not shown) compared to those of SMGs/ PGs (9–24%, Fig. 2l). It may cause less intense and delayed duct-related tissue injury, in our GVHD model.

Besides MHCII, several co-stimulatory molecules are required for interaction between antigen-presenting cells and T cells (Huppa et al., 2003). Among these molecules, intercellular adhesion molecule 1 (ICAM-1) and E-selectin were expressed on ducts of GVHD patients (Hiroki et al., 1996). In our microarray data, ICAM-1 expression was upregulated in GVHD group (not shown). However, on immunostained sections, ICAM-1 was expressed mainly in vascular endothelial cells, stroma, and infiltrating cells.

We think chemokines could be also crucial to explain contribution of ductal epithelial cells for the induction of salivary gland injury, because many reports suggest that chemokine secretion from irradiated skin, lung, and gut epithelium trigger tissue injury (Coghill et al., 2011; Wysocki et al., 2005). In our results, expression of CXCL9, CXCL10, and CCL5 were detected in not only GVHD but also irradiated control rats by immunostaining. However, at least mRNA of CCL5 was upregulated in GVHD rats analyzed with microarray and qPCR. It is possible that ductal epithelial cells secrete certain amount of chemokines constitutively. Such expression may induce infiltration and activation of donor T cells at early phase of the disease, and once T cell infiltration occurred, T cells secrete interferon-gamma to enhance further chemokine expression from ductal epithelial cells. Such interaction between ducts and T cells can be a positive feedback to enhance tissue injury.

In our observations, salivary gland injury occurred primarily in acinar areas, despite aberrant expression of MHCII and chemokines of ductal epithelial cells. Although exact mechanism is unknown, there are reduction of the acinar parenchyma while intraglandular ducts exhibit hyperplasia of the lining cells in Sjögren's syndrome (Barone et al., 2015). And factors like metalloproteinases are also reported to affect susceptibility of acini (Perez et al., 2005). These facts suggest that acinar cells are more susceptible to tissue injury than ductal cells in inflammatory diseases.

In our experiments, SLGs always showed minimal sign of injury. Similar to lacrimal glands, we noticed that density of ducts was narrower in the SLGs than that of SMGs and PGs (Fig. 2l). These results strongly suggest proportion of ductal areas correlated well with degree of tissue injury.

In conclusion, we discovered several findings which strongly suggest ductal epithelial cells are key enhancers for salivary gland injury. At least, ductal epithelial cells in salivary glands are sources of chemokines, and ducts are focal targets of infiltrating donor cells. Although direct evidence for antigen presentation and cell activation between MHCII-positive ductal epithelial cells and infiltrating donor cells are still to be found, our results should inform and promote further research on this important, but poorly studied complication of GVHD.

Acknowledgements

References

Alborghetti MR, Correa ME, Adam RL, Metze K, Coracin FL, de Souza CA, Cintra ML: Late effects of chronic graft-vs.-host disease in minor salivary glands. J Oral Pathol Med *34*: 486-493 (2005).

Barone F, Campos J, Bowman S, Fisher BA: The value of histopathological examination of salivary gland biopsies in diagnosis, prognosis and treatment of Sjogren's Syndrome. Swiss Med Wkly *145*: w14168 (2015).

Coghill JM, Sarantopoulos S, Moran TP, Murphy WJ, Blazar BR, Serody JS: Effector CD4+ T cells, the cytokines they

generate, and GVHD: something old and something new. Blood *117*: 3268-3276 (2011).

Fiaschi M, Kolterud A, Nilsson M, Toftgard R, Rozell B: Targeted expression of GLI1 in the salivary glands results in an altered differentiation program and hyperplasia. Am J Pathol *179*: 2569-2579 (2011).

Ford W, Hunt S: The preparation and labelling of lymphocytes (Chapter 23). In: Handbook of Experimental Immunology, 3rd edn, (Weir DM, ed.), Blackwell Scientific Publications, 1978 (p. 23.21-23.22)

Hayashi Y, Haneji N, Hamano H: Cytokine gene expression and autoantibody production in Sjogren's syndrome of MRL/lpr mice. Autoimmunity *23*: 269-277 (1996).

Hayashida JN, Nakamura S, Toyoshima T, Moriyama M, Sasaki M, Kawamura E, Ohyama Y, Kumamaru W, Shirasuna K: Possible involvement of cytokines, chemokines and chemokine receptors in the initiation and progression of chronic GVHD. Bone Marrow Transplant *48*: 115-123 (2013).

Hiroki A, Nakamura S, Shinohara M, Gondo H, Ohyama Y, Hayashi S, Harada M, Niho Y, Oka M: A comparison of glandular involvement between chronic graft-versus-host disease and Sjogren's syndrome. Int J Oral Maxillofac Surg *25*: 298-307 (1996).

Huppa JB, Davis MM: T-cell-antigen recognition and the immunological synapse. Nat Rev Immunol *3*: 973-983 (2003).

Imanguli MM, Atkinson JC, Mitchell SA, Avila DN, Bishop RJ, Cowen EW, Datiles MB, Hakim FT, Kleiner DE, Krumlauf MC, Pavletic SZ: Salivary gland involvement in chronic graft-versus-host disease: prevalence, clinical significance, and recommendations for evaluation. Biol Blood Marrow Transplant *16*: 1362-1369 (2010).

Kitazawa Y, Ueta H, Hunig T, Sawanobori Y, Matsuno K: A novel multicolor immunostaining method using ethynyl deoxyuridine for analysis of in situ immunoproliferative response. Histochem Cell Biol *144*: 195-208 (2015).

Lindahl G, Lonnquist B, Hedfors E: Lymphocytic infiltration and HLA-DR expression of salivary glands in bone marrow transplant recipients: a prospective study. Clin Exp Immunol *72*: 267-273 (1988).

Mantovani A, Bonecchi R, Locati M: Tuning inflammation and immunity by chemokine sequestration: decoys and more. Nat Rev Immunol *6*: 907-918 (2006).

Nagler RM, Nagler A: Salivary gland involvement in graft-versus-host disease: the underlying mechanism and implicated treatment. Isr Med Assoc J *6*: 167-172 (2004).

Nelson DA, Manhardt C, Kamath V, Sui Y, Santamaria-Pang A, Can A, Bello M, Corwin A, Dinn SR, Lazare M, Gervais EM, Sequeira SJ, Peters SB, Ginty F, Gerdes MJ, Larsen M: Quantitative single cell analysis of cell population dynamics during submandibular salivary gland development and differentiation. Biol Open *2*: 439-447 (2013).

Perez P, Kwon YJ, Alliende C, Leyton L, Aguilera S, Molina C, Labra C, Julio M, Leyton C, Gonzalez MJ: Increased acinar damage of salivary glands of patients with Sjogren's syndrome is paralleled by simultaneous imbalance of matrix metalloproteinase 3/tissue inhibitor of metalloproteinases 1 and matrix metalloproteinase 9/tissue inhibitor of metalloproteinases 1 ratios. Arthritis Rheum *52*: 2751-2760 (2005).

Prochorec-Sobieszek M, Nasilowska-Adamska B, Szumera-Cieckiewicz A, Tomaszewska A, Halaburda K, Szczepinski A, Szymanska-Giemza O, Ziarkiewicz-Wroblewska B, Marianska B: The significance of oral labial biopsy in hepatic graft-versus-host disease diagnosis in patients following allogeneic hematopoietic stem cell transplantation—a preliminary report. Ann Transplant *17*: 85-92 (2012).

Raimondi AR, Vitale-Cross L, Amornphimoltham P, Gutkind JS, Molinolo A: Rapid development of salivary gland carcinomas upon conditional expression of K-ras driven by the cytokeratin 5 promoter. Am J Pathol *168*: 1654-1665 (2006).

Sawanobori Y, Ueta H, Dijkstra CD, Park CG, Satou M, Kitazawa Y, Matsuno K: Three distinct subsets of thymic epithelial cells in rats and mice defined by novel antibodies. PLoS One *9*: e109995 (2014).

Soares AB, Faria PR, Magna LA, Correa ME, de Sousa CA, Almeida OP, Cintra ML: Chronic GVHD in minor salivary glands and oral mucosa: histopathological and immunohistochemical evaluation of 25 patients. J Oral Pathol Med *34*: 368-373 (2005).

Soares TC, Correa ME, Cintra GF, Miranda EC, Cintra ML: The impact of morphological and immunohistological changes in minor salivary glands on the health of the oral cavity in HSCT patients. Bone Marrow Transplant *48*: 1525-1529 (2013).

Steiniger B, Falk P, Lohmuller M, van der Meide PH: Class II MHC antigens in the rat digestive system. Normal distribution and induced expression after interferon-gamma treatment in vivo. Immunology *68*: 507-513 (1989).

Steiniger B, Falk P, Van der Meide PH: Interferon-gamma in vivo. Induction and loss of class II MHC antigens and immature myelomonocytic cells in rat organs. Eur J Immunol *18*: 661-669 (1988).

Takacs L, Szende B, Rot A, Diamanstein T: Expression of MHC class II antigens on bile duct epithelium in experimental graft versus host disease. Clin Exp Immunol *60*: 449-456 (1985).

Takaya M, Ichikawa Y, Shimizu H, Uchiyama M, Moriuchi J, Arimori S: Expression of MHC class II antigens and other T cell activation antigens on T cells and salivary duct epithelial cells in the salivary gland of cases of Sjogren's syndrome. Tokai J Exp Clin Med *15*: 27-33 (1990).

Tanaka T, Tahara-Hanaoka S, Nabekura T, Ikeda K, Jiang S, Tsutsumi S, Inagaki T, Magoori K, Higurashi T, Takahashi H, *et al.*: PPARbeta/delta activation of CD300a controls intestinal immunity. Sci Rep *4*: 5412 (2014).

Wang H, Asavaroengchai W, Yeap BY, Wang MG, Wang S, Sykes M, Yang YG: Paradoxical effects of IFN-gamma in graft-versus-host disease reflect promotion of lymphohematopoietic graft-versus-host reactions and inhibition of epithelial tissue injury. Blood *113*: 3612-3619 (2009).

Wysocki CA, Panoskaltsis-Mortari A, Blazar BR, Serody JS: Leukocyte migration and graft-versus-host disease. Blood *105*: 4191-4199 (2005).

Yang YG, Wang H, Asavaroengchai W, Dey BR: Role of Interferon-gamma in GVHD and GVL. Cell Mol Immunol *2*: 323-329 (2005).

Zhou S, Ueta H, Xu XD, Shi C, Matsuno K: Predominant donor CD103+CD8+ T cell infiltration into the gut epithelium during acute GvHD: a role of gut lymph nodes. Int Immunol *20*: 385-394 (2008).